Ocean Modelling 32 (2010) 188–204

Contents lists available at ScienceDirect

Ocean Modelling

journal homepage: www.elsevier.com/locate/ocemod

Parameterization of ocean eddies: Potential vorticity mixing, energetics and Arnold's first stability theorem

David P. Marshall [a,*], Alistair J. Adcroft [b]

[a] Atmospheric, Oceanic and Planetary Physics, Clarendon Laboratory, Parks Road, Oxford OX1 3PU, United Kingdom
[b] Atmospheric and Oceanic Sciences Program, Princeton University, 300 Forrestal Road, Sayre Hall, Princeton, NJ 08544, United States

ARTICLE INFO

Article history:
Received 6 July 2009
Received in revised form 28 January 2010
Accepted 1 February 2010
Available online 8 February 2010

Keywords:
Oceanic eddies
Parameterization
Potential vorticity
Energy budget
Stability

ABSTRACT

A family of eddy closures is studied that flux potential vorticity down-gradient and solve an explicit budget for the eddy energy, following the approach developed by Eden and Greatbatch (2008, Ocean Modelling). The aim of this manuscript is to demonstrate that when energy conservation is satisfied in this manner, the growth or decay of the parameterized eddy energy relates naturally to the instability or stability of the flow as described by Arnold's first stability theorem. The resultant family of eddy closures therefore possesses some of the ingredients necessary to parameterize the gross effects of eddies in both forced-dissipative and freely-decaying turbulence. These ideas are illustrated through their application to idealized, barotropic wind-driven gyres in which the maximum eddy energy occurs within the viscous boundary layers and separated western boundary currents, and to freely-decaying turbulence in a closed barotropic basin in which inertial Fofonoff gyres emerge as the long-time solution. The result that these eddy closures preserve the relation between the growth or decay of eddy energy and the instability or stability of the flow provides further support for their use in ocean general circulation models.

1. Introduction

The parameterization of geostrophic eddies in ocean models has been an active area of research throughout the last four decades. Many early ocean general circulation models (OGCMs) represented eddies through simple diffusion of heat, salt and momentum (e.g., Bryan, 1969). However, it was recognized early on that eddy closures should be constructed around properties that are materially conserved by fluid parcels, such as potential vorticity, while also respecting larger-scale constraints such as conservation of energy and angular momentum (Green, 1970).

A major advance resulted from the family of eddy parameterizations initiated by Gent and McWilliams (1990). These can be viewed as representing baroclinic instability through the introduction of an "eddy-induced" or "bolus" velocity (Gent et al., 1995) which acts to flatten density surfaces. Crucially, because the eddies are represented purely through additional advection of tracers, the Gent and McWilliams eddy parameterization conserves the net volume of fluid contained between any two isopycnal surfaces. The removal of the spurious diapycnal water mass transformations associated has resulted in a long list of improvements in OGCMs (Danabasoglu et al., 1994).

The success of Gent and McWilliams naturally leads one to speculate whether incorporating additional conservation properties into eddy parameterizations may lead to further improvements. One important issue concerns the fate of the energy released to the eddy field through baroclinic instability, which might be dissipated through bottom drag (as implicitly assumed in Gent and McWilliams, 1990; also see Arbic and Scott, 2008), surface drag (Duhant and Straub, 2006; Zhai and Greatbatch, 2007), exchange of energy with internal waves (Polzin, 2008) and subsequent interior diapycnal mixing (Tandon and Garrett, 1996), lee wave generation and subsequent bottom-enhanced diapycnal mixing (Marshall and Naveira Garabato, 2008), exchange of energy with submesoscales (Capet et al., 2008), or in western boundary layers (Zhai et al., manuscript in preparation).

Alternatively the eddy energy might be returned to the mean flow. This scenario is consistent with the results of freely-decaying turbulence in closed basins, in which finite-amplitude Fofonoff gyres emerge as the equilibrium solution (Bretherton and Haidvogel, 1976; Salmon et al., 1976; Cummins, 1992; Wang and Vallis, 1994) or bathymetry-following flows in the case with variable bathymetry (Bretherton and Haidvogel, 1976; Salmon et al., 1976; Holloway, 1987). Moreover, banded zonal jets naturally emerge in many instances of forced and freely-decaying turbulence in zonally-reentrant domains (e.g., Rhines, 1975; Williams, 1978). These results can be understood as a consequence of the direct cascade of potential enstrophy and the indirect cascade of energy.

* Corresponding author.
E-mail addresses: marshall@atm.ox.ac.uk (D.P. Marshall), aadcroft@princeton.edu (A.J. Adcroft).

1463-5003/$ - see front matter © 2010 Elsevier Ltd. All rights reserved.
doi:10.1016/j.ocemod.2010.02.001

Thus in the limit of weak dissipation, potential enstrophy is always dissipated, whereas energy is quasi-conserved – see Salmon (1998) for an excellent discussion.

The idea that the geostrophic turbulence preferentially dissipates potential enstrophy while conserving energy has been incorporated into two turbulence closure models: the anticipated potential vorticity method (Sadorny and Basdevant, 1985) and the alpha model (e.g., Holm and Wingate, 2005). However, these are best viewed as methods to arrest the potential enstrophy cascade in a partially resolved geostrophic eddy field, rather than as a complete eddy parameterization (e.g., Vallis and Hua, 1988). Adcock and Marshall (2000) develop a simple eddy parameterization that fluxes potential vorticity down-gradient while conserving energy, which they apply to freely-decaying turbulence in an abyssal layer overlying a seamount. A key result of this study is that the amount of potential vorticity mixing depends critically on the energy available in the initial state. Put another way, complete potential vorticity homogenization by eddies (e.g., Rhines and Young, 1982) sometimes raises the energy of the mean state, and thus requires a finite transfer of energy from the eddy field as a prerequisite.

Most recently, Eden and Greatbatch (2008) have proposed an alternative approach to energy conservation in which an explicit budget is solved for the turbulent eddy energy (also see Canuto and Dubovikov, 2006). This results in a two-level eddy closure in which the strength of the eddy fluxes of potential vorticity depend not only on the mean gradients, but also on an eddy transfer coefficient which, in turn, is related to the eddy energy. Cessi (2008) proposes an analogous eddy closure for potential temperature fluxes in which local equilibrium is assumed between eddy energy sources and sinks.

In this contribution, we investigate the stability properties of eddy closures which both flux potential vorticity down-gradient and also solve an explicit budget for the eddy energy (as developed by Eden and Greatbatch). Our specific aims are:

- To demonstrate, when energy conservation is satisfied through an explicit eddy energy budget following the approach of Eden and Greatbatch, that the growth or decay of the parameterized eddy energy in a barotropic ocean is related naturally to the instability or stability of the flow as described by Arnold's first stability theorem; this is the major new result of our manuscript.
- To demonstrate that such closures can successfully develop localized regions of parameterized eddy energy within the separated western boundary currents of barotropic wind-driven gyres, as well as generate finite-amplitude Fofonoff gyres in freely-decaying barotropic turbulence.
- To extend the relation between the growth or decay of the parameterized eddy energy and the instability or stability of the flow to a stratified, quasigeostrophic ocean.

The connections between instability theory, eddy fluxes of potential vorticity, and conservation principles have been developed most completely in the series of papers by Killworth (1997, 1998, 2001, 2005), in which linear stability theory is applied to develop eddy closures. While eddies are far from linear (e.g., Canuto and Dubovikov, 2005), Killworth argues that linear theory provides analytical solutions to the equations of motion, which thus satisfy the relevant conservation principles, and for this reason its solutions provide useful guidance in the development of eddy closures. While we do not invoke linear theory in the present manuscript, our motivations are very much in tune with those of Peter Killworth. We are therefore delighted to be able to contribute to this commemorative issue dedicated to Peter's life and work.

The paper is structured as follows. In Section 2, the eddy closure is formulated for a barotropic ocean basin. In Section 3, the relation between the growth of the eddy energy and the instability of the flow is derived. In Section 4, the eddy closure is applied to wind-driven gyres and freely-decaying turbulence in a closed barotropic basin. In Section 5, it is shown that the relation between the growth of the eddy energy and the instability properties of the flow carries over to a stratified, quasigeostrophic ocean. Finally, in Section 6, our key findings and outstanding challenges are summarized.

2. Barotropic ocean

2.1. Equations of motion

First we restrict our attention to a barotropic ocean of uniform depth, this being the simplest framework within which eddy momentum fluxes and Coriolis effects are represented.

The time-filtered equations of motion consist of a momentum equation,

$$\frac{\partial \mathbf{u}}{\partial t} + \mathbf{k} \times q\mathbf{u} + \nabla B = \mathbf{F} - \mathbf{k} \times \overline{q'\mathbf{u}'} - \nabla \frac{\overline{\mathbf{u}' \cdot \mathbf{u}'}}{2}, \tag{1}$$

and the continuity equation,

$$\nabla \cdot \mathbf{u} = 0. \tag{2}$$

Here $\mathbf{u}$ is the velocity, $\mathbf{k}$ is a unit vertical vector,

$$q = f(y) + \frac{\partial v}{\partial x} - \frac{\partial u}{\partial y}$$

is the absolute vorticity, $f(y)$ is the planetary vorticity,

$$B = \frac{p}{\rho} + \frac{u^2 + v^2}{2}$$

is the Bernoulli potential, $\mathbf{F}$ represents all body forces (including any friction), (x, y) are the coordinates in the east- and northward directions and t is time. The remaining terms on the right-hand side represent the eddy momentum fluxes where primes indicate the eddy components of the flow and all other variables are assumed to have been time-filtered.

In this formulation, there are three eddy fields requiring parameterization: the two components of the eddy vorticity flux, $\overline{q'\mathbf{u}'}$, and the eddy kinetic energy, $\overline{\mathbf{u}'.\mathbf{u}'}$.[1]

2.2. Energetics

The mean energy equation can be written:

$$\frac{\partial}{\partial t}\left(\frac{\mathbf{u} \cdot \mathbf{u}}{2}\right) + \nabla \cdot (B\mathbf{u}) + \nabla \cdot \left(\frac{\overline{\mathbf{u}' \cdot \mathbf{u}'}}{2}\mathbf{u}\right) = \mathbf{u} \cdot \mathbf{F} - \mathbf{u} \cdot \mathbf{k} \times \overline{q'\mathbf{u}'}. \tag{3}$$

We can also form an eddy kinetic energy equation as follows. The transient momentum equation is

$$\frac{\partial \mathbf{u}'}{\partial t} + \mathbf{k} \times (q\mathbf{u}') + \mathbf{k} \times (q'\mathbf{u}) + \mathbf{k} \times (q'\mathbf{u}') + \nabla B' = \mathbf{F}'.$$

[1] Note that the gradient of the eddy kinetic energy is purely divergent (i.e., is curl-free) and unable to project onto the Eulerian acceleration, $\partial \mathbf{u}/\partial t$, which is purely rotational (i.e., is divergence-free). Thus the only eddy forcing that affects the evolution of the mean flow is associated with the eddy vorticity flux – this is consistent with the concept that the evolution of the mean flow can be determined by solving a vorticity equation, in which only the eddy vorticity flux appears. In contrast, the acceleration associated gradient of the eddy kinetic energy leads to a modified pressure field, but it has no impact on the evolution of the mean flow (see, for example, Hughes and Ash, 2001.)

Now taking the dot product with $\mathbf{u}'$ and rearranging, we obtain:

$$\frac{\partial}{\partial t}\left(\frac{\overline{\mathbf{u}'\cdot\mathbf{u}'}}{2}\right)+\nabla\cdot\overline{B'\mathbf{u}'}=\overline{\mathbf{u}'\cdot\mathbf{F}'}+\mathbf{u}\cdot\mathbf{k}\times\overline{q'\mathbf{u}'}. \tag{4}$$

The term $\mathbf{u}\cdot\mathbf{k}\times\overline{q'\mathbf{u}'}$, appearing with opposite signs in (3) and (4), represents the conversion of energy between the mean and eddy components. The term $\overline{\mathbf{u}'\cdot\mathbf{F}'}$ represents the forcing and dissipation of eddy energy through transient wind forcing and frictional drag. The remaining eddy term, $\nabla\cdot\overline{B'\mathbf{u}'}$, is the divergence of a flux and acts only to redistribute eddy energy.

Finally, we can define a streamfunction, ψ, for the flow such that $\mathbf{u}=\mathbf{k}\times\nabla\psi$. The conversion of energy between the mean and eddy components can then be rewritten as:

$$\mathbf{u}\cdot\mathbf{k}\times\overline{q'\mathbf{u}'}=\nabla\psi\cdot\overline{q'\mathbf{u}'}. \tag{5}$$

This result is central to the relations between closures for the eddy vorticity flux and the flow stability which we will derive in Section 3.

2.3. Eddy flux of vorticity

In two-dimensional turbulence, enstrophy cascades to small scales where it is ultimately dissipated (e.g., Green, 1970). This can be captured in an eddy parameterization by assuming a down-gradient closure for the vorticity flux to within an arbitrary rotational gauge:

$$\overline{q'\mathbf{u}'}=-\kappa\nabla q+\mathbf{k}\times\nabla\lambda. \tag{6}$$

Here we allow the eddy transfer coefficient, κ, to vary spatially, although we assume it is always positive, $\kappa>0$. Note that this latter assumption does not require the eddy vorticity flux to be locally down-gradient due to the presence of the rotational gauge.

We also impose a boundary condition on the normal component of the eddy flux,

$$\mathbf{n}\cdot\overline{q'\mathbf{u}'}=0, \tag{7}$$

which is achieved most conveniently by setting $\kappa=\lambda=0$ on the boundaries in (6).

2.4. Closure for the eddy diffusivity

Having derived a relation for the conversion of energy between the mean and eddy components, (5), we now need to develop a closure for the eddy transfer coefficient, κ. There are two obvious choices.

The first choice, following Green (1970), Stone (1972), and, in the present context, Eden and Greatbatch (2008), is to set

$$\kappa=\alpha L_{\mathrm{eddy}}U_{\mathrm{eddy}}=\alpha L_{\mathrm{eddy}}(2E)^{1/2}, \tag{8}$$

where

$$E=\frac{\overline{\mathbf{u}'\cdot\mathbf{u}'}}{2}=\frac{U_{\mathrm{eddy}}^2}{2}$$

is the eddy kinetic energy and U_{eddy} is a root-mean squared eddy velocity. L_{eddy} is a prescribed eddy mixing length scale which one might identify with the Rhines scale (Rhines, 1975) or, more generally in a baroclinic ocean, with the Rossby deformation radius or the width of the baroclinic zone – see Visbeck et al. (1997) and Eden and Greatbatch (2008) for related discussions. Following Green (1970), we set α to be a dimensionless constant of order 10^{-2}. In contrast, Eden and Greatbatch choose $\alpha=1$; however, we find a smaller value necessary to obtain realistic eddy transfer coefficients and eddy kinetic energies in numerical calculations reported in Section 4.

The second choice is to set

$$\kappa=\gamma\mathscr{T}_{\mathrm{eddy}}U_{\mathrm{eddy}}^2=2\gamma\mathscr{T}_{\mathrm{eddy}}E, \tag{9}$$

where $\mathscr{T}_{\mathrm{eddy}}$ is an eddy turnover time-scale and γ is again a dimensionless constant.

2.5. Remaining terms in the eddy energy equation

The eddy energy Eq. (4) can now be rewritten

$$\frac{\partial E}{\partial t}=-\kappa\nabla\psi\cdot\nabla q-\nabla\cdot(\overline{B'\mathbf{u}'}+\lambda\mathbf{u})+\overline{\mathbf{u}'\cdot\mathbf{F}'}. \tag{10}$$

The first term on the right-hand side of (10) represents the net mean-eddy energy conversion and will be discussed further in Section 3. The final term represents the source of eddy energy associated with transient forcing (which is likely significant in the real world but not considered further here) and the sink of eddy energy associated with friction which we parameterize through a simple Newtonian damping. The term $\nabla\cdot\overline{B'\mathbf{u}'}$ represents dispersion of eddy energy and may involve a myriad of processes such as Rossby wave propagation — an excellent discussion is given in Eden and Greatbatch (2008). Here we follow Eden and Greatbatch and parameterize the eddy dispersion term as a simple diffusion of eddy energy, albeit at a higher rate, κ_E. We find that taking $\kappa_E=\kappa$ generally leads to insufficient dispersion of eddy energy, which instead remains excessively confined to the region of eddy energy generation when compared with eddy-resolving calculations.

Thus:

$$\frac{\partial E}{\partial t}=-\kappa\nabla\psi\cdot\nabla q+\nabla\cdot(\kappa_E\nabla E-\lambda\mathbf{u})-rE \tag{11}$$

where r is an inverse time scale for eddy energy decay.

Comparing the eddy closure (6) with the mean energy Eq. (3), it is tempting to identify at least part of the rotational component of the eddy potential vorticity flux with the eddy kinetic energy. Thus we set:

$$\lambda=\frac{\overline{\mathbf{u}'\cdot\mathbf{u}'}}{2}\Rightarrow\overline{q'\mathbf{u}'}=-\kappa\nabla q+\mathbf{k}\times\nabla\left(\frac{\overline{\mathbf{u}'\cdot\mathbf{u}'}}{2}\right).$$

This implies anticyclonic circulation of the total vorticity flux around regions of eddy activity, broadly consistent with analysis of Marshall and Shutts (1981). Substituting for λ in the eddy energy equation suggests that this term is (at least in part) associated with the advection of eddy energy by the mean flow:

$$\frac{\partial E}{\partial t}+\mathbf{u}\cdot\nabla E=-\kappa\nabla\psi\cdot\nabla q+\nabla\cdot(\kappa_E\nabla E)-rE. \tag{12}$$

3. Relation to Arnold's first stability condition

3.1. Parameterized stability condition

Substituting for the eddy flux of potential vorticity flux (6) in (5), the conversion of energy between the mean and eddy components is:

$$\mathbf{u}\cdot\mathbf{k}\times\overline{q'\mathbf{u}'}=-\kappa\nabla\psi\cdot\nabla q-\nabla\cdot(\lambda\mathbf{u}). \tag{13}$$

The second term on the right-hand side of (13) is the divergence of a flux and hence represents a further redistribution of energy. Thus, only the first term on the right-hand side of (13) represents a *net* energy conversion. This first term can, in turn, be written in the form

$$\boxed{\text{energy conversion}=-\kappa\nabla\psi\cdot\nabla q=-\kappa\frac{\partial q}{\partial\psi_\perp}\,\mathbf{u}\cdot\mathbf{u},} \tag{14}$$

where

$$\frac{\partial q}{\partial\psi_\perp}=\frac{\nabla q\cdot\nabla\psi}{\nabla\psi\cdot\nabla\psi}$$

represents the rate of change of the vorticity with respect to the streamfunction in the direction perpendicular to the streamlines. This result indicates that the present family of eddy closures satisfy an analogue of the first nonlinear stability theorem due to Arnold (1965).

Specifically, for a barotropic ocean, Arnold's condition states that if $dq/d\psi > 0$ everywhere, then the flow is unconditionally stable to finite-amplitude perturbations. With the family of eddy closures considered here, if $\partial q/\partial\psi_\perp > 0$, then eddy energy is locally converted to mean energy; conversely, if $\partial q/\partial\psi_\perp < 0$ then mean energy is locally converted to eddy energy. While these results do not ensure local eddy energy decay or growth due to the presence of additional terms in the energy budget that can be written as the divergence of fluxes, these latter terms are easily removed by integrating over the domain.

Thus: $\partial q/\partial\psi_\perp > 0$ *everywhere is a sufficient condition for stability in the parameterized model*, in the sense that the integrated eddy energy is guaranteed decay at the expense of mean energy. Conversely, $\partial q/\partial\psi_\perp < 0$ *somewhere is a necessary condition for instability in the parameterized model*, in the sense that the integrated eddy energy may be able to grow at the expense of mean energy. This is our parameterized analogue of Arnold's first stability theorem.

3.2. Physical interpretation: conservation of pseudoenergy

The physical origin of Arnold's first stability theorem, and its role in the present eddy closure, can be elucidated by considering the conservation of pseudoenergy (see, e.g., Salmon, 1998).

In the inviscid fluid equations, conservations laws are related to symmetries in the associated Hamiltonian. In particular, if the Hamiltonian is symmetric under time transformations, this gives rise to energy conservation. One can also write down an "averaged Hamiltonian" when the flow is separated into a mean flow (which, for the purpose of the present discussion is assumed steady and hence $q = q(\psi)$), and transient eddies. If the averaged Hamiltonian is symmetric under time transformations, then this gives rise to conservation of the basin-integrated pseudoenergy,

$$P = \iint \left(\frac{\overline{\mathbf{u}' \cdot \mathbf{u}'}}{2} + \left(\frac{dq}{d\psi}\right)^{-1} \frac{\overline{q'^2}}{2} \right) dxdy. \tag{15}$$

Note that eddy energy is not conserved since energy is exchanged between the eddies and the mean flow.

Arnold's first stability theorem follows because when $dq/d\psi > 0$ everywhere, conservation of pseudoenergy means that the eddy energy can grow only at the expense of eddy enstrophy, and is bounded in magnitude by the initial pseudoenergy (Vallis, 2006).

While eddy enstrophy is not carried as a prognostic variable in the present closure, the growth of eddy enstrophy is implicit in the down-gradient eddy vorticity flux:

$$\begin{aligned} \frac{\partial}{\partial t} \iint \frac{\overline{q'^2}}{2} dxdy &= -\iint \overline{q'\mathbf{u}'} \cdot \nabla q dxdy = \iint \kappa \nabla q \cdot \nabla q dxdy \\ &= -\iint \frac{dq}{d\psi} (\text{energy conversion}) dxdy. \end{aligned} \tag{16}$$

Thus as vorticity is fluxed down-gradient and eddy enstrophy grows, the eddy energy is guaranteed to decay if $dq/d\psi > 0$ everywhere, and may grow if $dq/d\psi < 0$ somewhere. Moreover the mean-to-eddy conversion terms for enstrophy and energy are proportional to each other with proportionality constant $dq/d\psi$, consistent with conservation of pseudoenergy.[2]

[2] Note that while conservation of pseudoenergy requires the mean flow to be stationary, the result that the ratio of the mean-to-eddy conversion terms for enstrophy and energy is $-\partial q/\partial\psi_\perp = -\nabla q \cdot \nabla\psi / \nabla\psi \cdot \nabla\psi$ holds more generally.

3.3. Local eddy energy growth rates

It is instructive to write down local approximations for the growth of the eddy energy for each of the closures for the eddy diffusivity in the artificial limit that: (i) the background flow evolves slowly; and (ii) diffusion, advection and other dispersion of eddy energy can be neglected. In the following, we do include the effect of eddy damping, allowing for local equilibration between eddy growth and damping, as assumed in the baroclinic eddy closure of Cessi (2008). The undamped eddy growth rates are obtained by taking the limit $r \to 0$ is the following expressions.

In the case of (8), we have

$$\frac{\partial E}{\partial t} \approx -2^{1/2} \alpha L_{\text{eddy}} \mathbf{u} \cdot \mathbf{u} \frac{\partial q}{\partial \psi_\perp} E^{1/2} - rE$$

giving

$$\left(E^{1/2} + \frac{2^{1/2} \alpha L_{\text{eddy}} \mathbf{u} \cdot \mathbf{u}}{r} \frac{\partial q}{\partial \psi_\perp} \right) = \left(E_0^{1/2} + \frac{2^{1/2} \alpha L_{\text{eddy}} \mathbf{u} \cdot \mathbf{u}}{r} \frac{\partial q}{\partial \psi_\perp} \right) \exp\left\{ -\frac{rt}{2} \right\}, \tag{17}$$

where E_0 is the energy at time $t = 0$. This gives growth of the eddy energy when $\partial q/\partial\psi_\perp < 0$, equilibrating on the eddy damping time scale, $1/r$, and to decay of the eddy energy when $\partial q/\partial\psi_\perp > 0$, over a finite time,

$$t = \frac{2}{r} \log\left\{ 1 + \frac{E_0^{1/2} r}{2^{1/2} \alpha L_{\text{eddy}} \mathbf{u} \cdot \mathbf{u}} \left(\frac{\partial q}{\partial \psi_\perp} \right)^{-1} \right\}.$$

In the case of (9), we instead have

$$\begin{aligned} \frac{\partial E}{\partial t} &\approx -\left(r + 2\gamma \mathscr{T}_{\text{eddy}} \mathbf{u} \cdot \mathbf{u} \frac{\partial q}{\partial \psi_\perp} \right) E \Rightarrow E \\ &= E_0 \exp\left\{ -\left(r + 2\gamma \mathscr{T}_{\text{eddy}} \mathbf{u} \cdot \mathbf{u} \frac{\partial q}{\partial \psi_\perp} \right) t \right\}, \end{aligned} \tag{18}$$

i.e., the eddy energy grows or decays exponentially depending on the sign of $\partial q/\partial\psi_\perp$ and the magnitude of the eddy energy damping. In this case, equilibration can only occur through changes to the mean flow (removing the source of the eddy growth), through advection/diffusion of the eddy energy (or other eddy energy dispersion processes), or through a higher-order energy dissipation term.

We are unaware of any direct correspondence between the functional forms of (17) and (18) and growth rates inferred from detailed stability analyses. Nevertheless, that eddies grow/decay most rapidly in regions that the background flow is strong and $\partial q/\partial\psi_\perp$ is negative/positive is broadly consistent with general experience. Marshall and Marshall (1992) identify the no-slip boundaries layers in the western boundary currents and the core of the separated inertial jet between the subtropical and subpolar gyres as regions of strongly negative $\partial q/\partial\psi_\perp$; both are known to be regions of eddy energy growth (e.g., Berloff and McWilliams, 1999 and Holland and Rhines, 1980, respectively). Conversely, in freely-decaying turbulence in a rectangular basin, the equilibrium solution is known to be a pair of Fofonoff gyres in which all of the initial eddy energy is converted to mean energy and $dq/d\psi > 0$ (Bretherton and Haidvogel, 1976; Wang and Vallis, 1994).

We wish to reiterate that the equilibrium eddy energies and growth rates will almost certainly be modified by the advection, diffusion and other dispersion of eddy energy. These processes are completely neglected in the preceding discussion and hence the actual growth/decay of eddy energy will almost certainly differ from the idealized limits considered above.

4. Numerical examples

In this section, we aim to illustrate the ideas developed in Sections 2 and 3 with numerical solutions. We apply the eddy closure to both the wind-driven circulation in a rectangular basin and the emergence of Fofonoff gyres in freely-decaying turbulence. We do not attempt to provide a comprehensive validation of the closure since it contains many degrees of freedom associated with the dispersion and dissipation of eddy energy that require extensive further study. Rather we focus on the relation between the growth of the eddy energy and the instability of the background flow, making qualitative comparisons between results with parameterized and explicitly-resolved eddies.

4.1. Model details

We solve for the circulation in a rectangular barotropic basin with boundaries at $x, y = \pm L$, dimension $2L = 4000$ km. The basin depth is set at 500 m, representing a typical vertical scale of wind-driven circulation in the ocean. The Coriolis parameter is assumed to vary linearly with latitude with $\beta = df/dy = 2\times 10^{-11}$ m^{-1} s^{-1} (in the barotropic model, solutions are independent of the mean value of the Coriolis parameter).

Dissipation is through Newtonian damping of eddy kinetic energy as detailed in (11) with a coefficient $r = 10^{-7}$ s^{-1} in the wind-driven calculations; we leave the eddy energy undamped and set $r = 0$ in the freely-decaying turbulence simulations. Diffusion of vorticity is through the parameterized eddy diffusivity, κ, which is solved for explicitly using (14) and (8), and through biharmonic diffusion with a dissipation coefficient $A = \Delta x^4/(3\times 10^6\mathrm{s})$ where Δx is the grid spacing. Eddy energy is diffused at a rate $\kappa_E = 10^4$ m^2 s^{-2}, the relatively large value of which we find necessary to ensure sufficient dispersion of the eddy energy, which otherwise remains far too tightly confined to the region of eddy energy growth compared with eddy-resolving calculations. For the remaining physical parameters we set $\alpha = 0.01, L_{\mathrm{eddy}} = 2\times 10^5$ m. These choices have been made through trial and error to give a plausible distribution of eddy energy and realistic values for the eddy diffusivity of vorticity compared with eddy-resolving calculations.

On the boundaries we specify no-normal flow, $\psi = 0$, and either $\nabla^2\psi = 0$ for free-slip or $\nabla_\perp\psi = 0$ for no-slip conditions. In Section 4.4, we consider an alternative slippery boundary condition in which the diffusive flux of vorticity through the boundary vanishes. The biharmonic diffusion operator additional requires a higher-order boundary condition for which we set $\nabla^4\psi = 0$.

A slip boundary condition is not applied to the parameterized eddy energy; rather we simply set $\kappa_E = 0$ on the boundaries such that the eddy dispersion term does not modify the total eddy energy. In this sense, the parameterized eddy energy equation is inconsistent with the mean momentum equation. However, in some preliminary experiments in which we applied a no-slip condition to the parameterized eddy energy, the results were not qualitatively different (except that the overall eddy energy was slightly reduced).

The integrations with parameterized eddies are on a 128×128 grid, giving a grid spacing of $\Delta x = 31.25$ km; the eddy-resolving integrations are on a 256×256 with a grid spacing of $\Delta x = 15.625$ km. The integrations with parameterized eddies are able to resolve some of the effects of interia and some weakly-energetic transient motions, but do not generate a turbulent eddy field.

The equations of motion are solved in vorticity–streamfunction form. The eddy kinetic energy grid points are staggered from the streamfunction and vorticity, the former being held at the center of the grid cells and the latter at the corners (which coincide with the coastlines). Vorticity advection is discretized using an Arakawa Jacobian. The remaining terms are discretized using standard centered finite differences. Time-stepping is with a leap-frog scheme and a Robert- -Aselin filter (strength 10^{-2}) to prevent divergence of adjacent time steps. The dissipation and eddy diffusion terms are backward-differenced for numerical stability. For further details of the numerics, the reader is referred to Tansley and Marshall (2001).

4.2. Wind-driven gyres: free-slip boundaries

We present solutions for wind-driven gyres with free-slip and no-slip boundary conditions respectively. Forcing is through a zonal wind stress which varies sinusoidally with latitude:

$$\tau = \tau_0 \cos\left(\frac{\pi y}{L}\right)\mathbf{i}$$

where $\tau_0 = 0.1$ N m^{-2}. The solutions are integrated from a state of rest for 10 model years.

Firstly we consider a free-slip solution. In Fig. 1 we show snapshots of the streamfunction, vorticity, parameterized eddy energy and mean-to-eddy energy conversion after 10 years. The solution contains subtropical and subpolar gyres, with fairly intense inertial recirculation sub-gyres (the peak gyre transports are around 60 Sv) and a separated jet at the inter-gyre boundary that fluctuates alternately north and south. The solution contains transient motion throughout the basin, but with no irreversible mixing of vorticity through the formation and subsequent erosion of vorticity filaments. Irreversible mixing of vorticity is thus through the parameterized eddy diffusion.

The parameterized eddy kinetic energy has a maximum at the inter-gyre boundary, displaced slightly downstream of the inertial recirculation sub-gyres. The eddy energy decays to small values in the far field, with the spatial extent of the region of large eddy kinetic energy being a function primarily of the rate at which the eddy energy is diffused and, to a lesser extent, advection of eddy energy by the mean flow.

In contrast, energy conversion from the mean component to the parameterized eddy component (14) is mostly confined to an extremely narrow strip at the inter-gyre boundary, with some eddy energy generation also present adjacent to the western boundary. These are the regions in which one finds both large negative values of $\partial q/\partial\psi_\perp$ (e.g., Marshall and Marshall, 1992) and large mean flows and, therefore, large energy growth by (14). There is some weak parameterized eddy-to-mean energy conversion (negative values in panel (d)) within the mean core of the western boundary currents, and to the north and south of the region of maximum eddy energy growth within the separated jet. These are regions in which $\partial q/\partial\psi_\perp > 0$, as one would expect for an inertial boundary current solution (Fofonoff, 1954; Marshall and Marshall, 1992); in these regions, energy is back-scattered to the mean flow, a point that is pursued further in Section 4.4.

In Figs. 2 and 3, we show equivalent fields from the eddy-resolving integration. In order to allow the eddies to dissipate in an analogous manner to the case with parameterized eddies, we include a linear friction in this integration with a coefficient 0.5×10^{-7} s^{-1} (it is easily shown that this leads to Newtonian damping of eddy energy at the same rate $r = 10^{-7}$ s^{-1} employed in the integration with parameterized eddies). The figure panels show the mean streamfunction, vorticity and eddy energy, and the mean-to-eddy energy conversion, averaged over two year intervals: years 5–6 and years 9–10, respectively. The mean-to-eddy energy conservation is defined as

$$\overline{\mathbf{u}}\cdot\mathbf{k}\times\overline{q'\mathbf{u}'}_{\mathrm{div}} \tag{19}$$

where the eddy vorticity flux has been decomposed into divergent and rotational components (both satisfying a no-normal flux

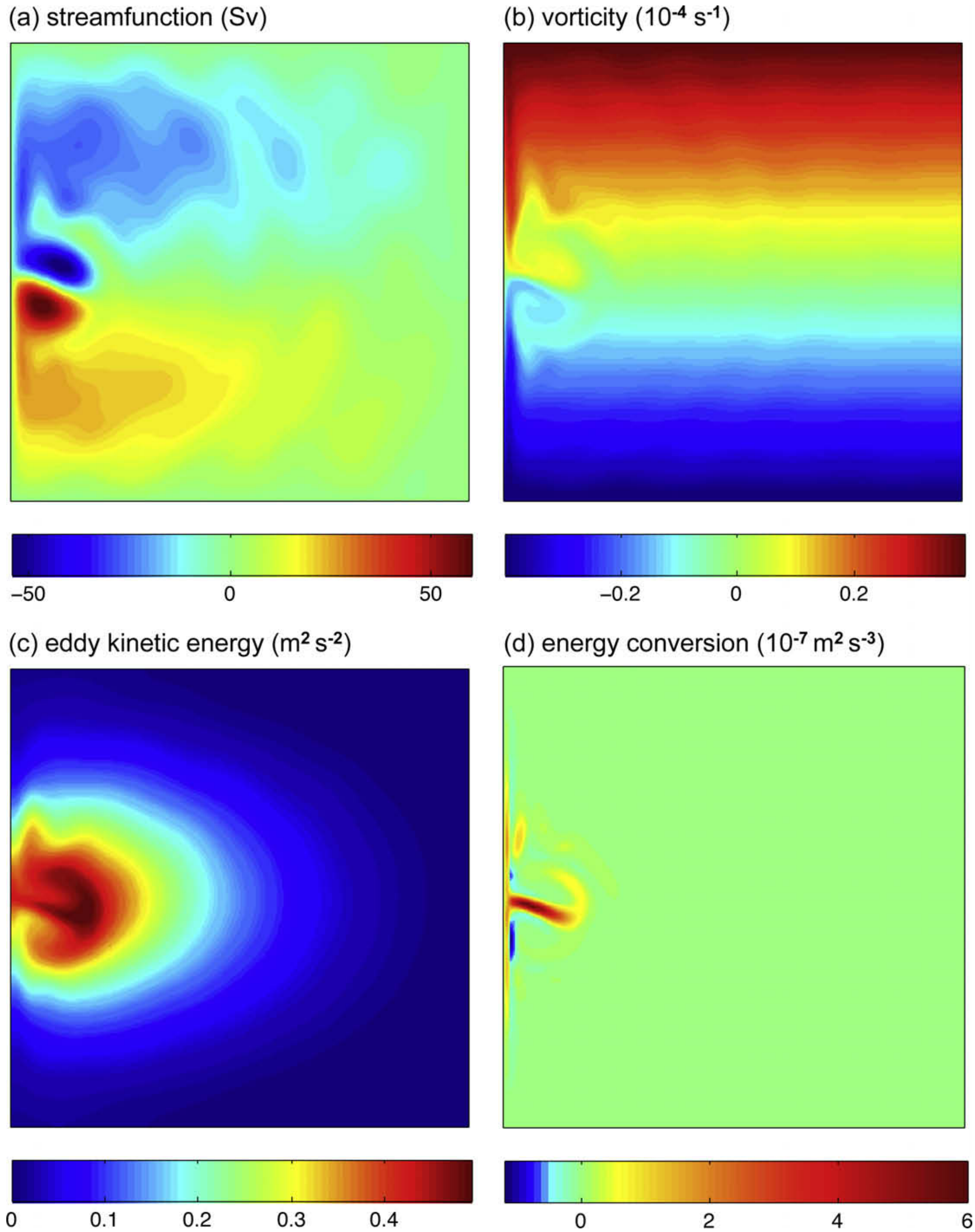

Fig. 1. Wind-driven gyres with free-slip boundary conditions and parameterized eddies. The panels show snapshots over the entire domain, after 10 years of integration from a rest state, of: (a) transport streamfunction, $H\psi$ (Sv); (b) absolute vorticity $(10^{-4}\ \mathrm{s}^{-1})$; (c) parameterized eddy kinetic energy $(\mathrm{m}^2\ \mathrm{s}^{-2})$; (d) mean-to-eddy energy conversion, $-\kappa\nabla\psi\cdot\nabla q$ $(10^{-7}\ \mathrm{m}^2\ \mathrm{s}^{-3})$. The eddy diffusivity is proportional to the square root of the eddy kinetic energy, with a peak value of roughly 2000 $\mathrm{m}^2\ \mathrm{s}^{-1}$.

boundary condition – see Roberts and Marshall, 2000 for further discussion). This decomposition is made is remove the largest component of the eddy flux, directed around contours of eddy energy (cf. Marshall and Shutts, 1981), consistent with the parameterized mean-to-eddy conversion being defined in terms of the component of the eddy vorticity flux directed down the mean vorticity gradient in (14).[3]

[3] Note, also, that an explicit time-averaging operator is included in the definition of the mean velocity in (19) since, in contrast to the case with parameterized eddies where the "mean" velocity is defined at every time step, in the case with explicit eddies it is obtained as the time-average over a two-year window.

Over the first time-interval, years 5–6 (Fig. 2), the mean flow has many qualitative similarities with the solution after 10 years in the case with parameterized eddies (Fig. 1). The eddy energy field is roughly a factor of two stronger in the integration with explicit eddies, but the distribution of eddy energy is broadly similar with somewhat enhanced eddy energy adjacent to the western boundary in the eddy-resolving case. The mean-to-eddy energy conversion in the eddy-resolving integration (Fig. 2d) has a qualitatively similar structure to that with parameterized eddies (Fig. 1d). The largest energy conversion is found in the separated jet at the inter-gyre boundary. The main difference in the eddy-resolving integration is a more extended region of eddy energy de-

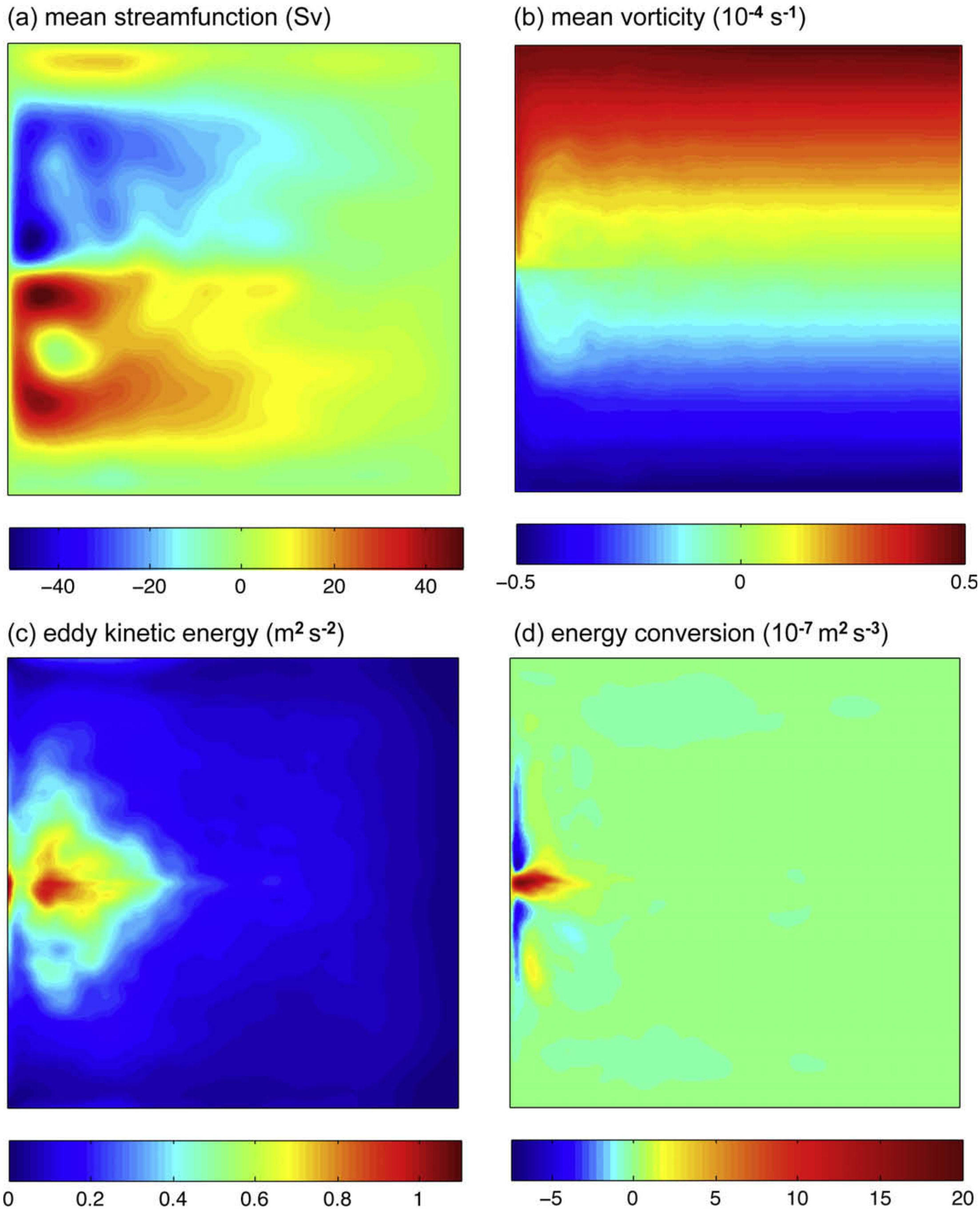

Fig. 2. Wind-driven gyres with free-slip boundary conditions and explicit eddies. The panels show a 2 year average over years 5–6 of integration from a rest state, of: (a) transport streamfunction, $H\overline{\psi}$ (Sv); (b) absolute vorticity (10^{-4} s^{-1}); (c) eddy kinetic energy (m^2 s^{-2}); (d) mean-to-eddy energy conversion, $\overline{\mathbf{u}} \cdot \mathbf{k} \times \overline{q'\mathbf{u}'}_{\mathrm{div}}$ (10^{-7} m^2 s^{-3}).

cay within the inertial western boundary currents where $\partial q/\partial \psi_\perp > 0$; there is also a hint of inertial Fofonoff gyres forming at the northern and southern flanks of the basin.

Over the second time-interval, years 9–10 (Fig. 3), the inertial Fofonoff gyres have grown to similar amplitude as the main gyres, such that there is now a four-gyre circulation (cf. Greatbatch and Nadiga, 2000). The pattern of eddy energy conversion in the center of the basin is qualitatively similar to that obtained over the earlier time interval, but with some additional structure over the northern and southern parts of the basin. Our parameterized eddy calculations appear to be unable to support the growth of substantial Fofonoff gyres with free-slip boundary conditions; however, these Fofonoff gyres are obtained if the free-slip condition is replaced by a hyper-slip boundary condition – this scenario is explored in freely-decaying turbulence simulations in Section 4.4.

The mean-to-eddy energy conversion term (19) in Figs. 2d and 3d has been calculated using the *divergent* component of the eddy vorticity flux. This is in keeping with the definition of the parameterized conversion term being in terms of the component of the eddy vorticity flux directed down the mean vorticity gradient (14). For completeness. in Fig. 4, we show the equivalent conversion terms calculated using the *full* eddy vorticity flux,

$$\overline{\mathbf{u}} \cdot \mathbf{k} \times \overline{q'\mathbf{u}'}.$$

There are significant differences between the two forms of the eddy conversion term, emphasising that the eddy conversion is

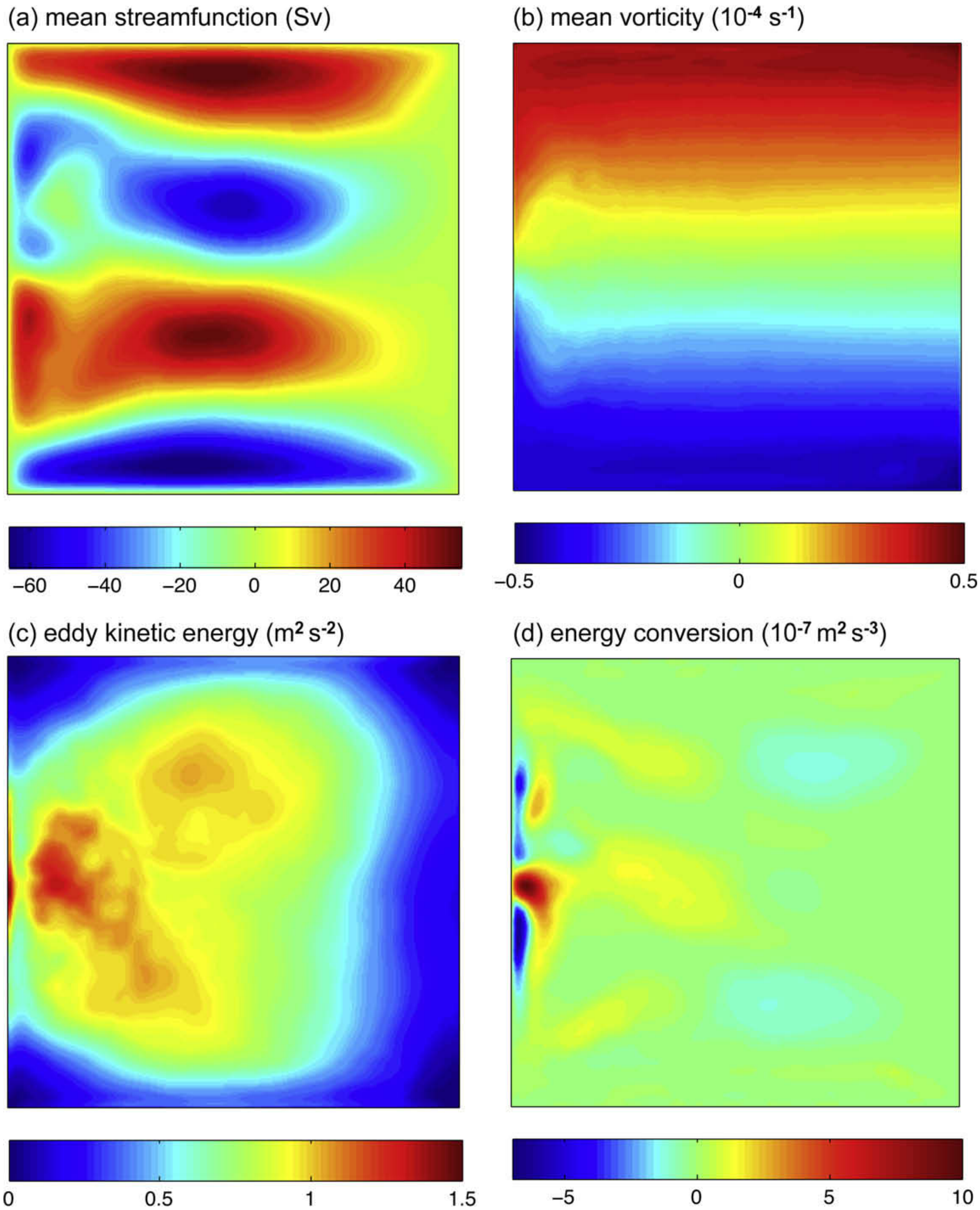

Fig. 3. As in Fig. 2 but averaged over years 9–10 of the integration.

uniquely defined only in the integral sense: any rotational eddy vorticity fluxes modify the mean-to-eddy energy conversion by a term which can be written as the divergence of a flux: this has no impact on the global energy conversion, although it can significantly modify local values. Nevertheless, the energy conversion defined in terms of the full eddy vorticity flux still has a maximum in the separated jet between the subtropical and subpolar gyres, albeit with alternate positive and negative values in the zonal direction. The fact that both forms of the energy conversion term produce maximum values in roughly the same location is because both the mean flow and eddy fluxes are largest in this inter-gyre region.

4.3. Wind-driven gyres: no-slip boundaries

We now present a no-slip solution. In Fig. 5 the equivalent fields to those in Fig. 1 are plotted after 10 years of integration in the case with no-slip boundaries and parameterized eddies. The main difference is that the inter-gyre jet and intense recirculation subgyres are replaced by more dissipative western boundary currents. The gyre transports are broadly consistent with Sverdrup balance, with damped standing Rossby waves decaying away from the western boundary near the inter-gyre boundary. The eddy kinetic energy is broadly similar to the free-slip solution, with the maximum slightly increased but the eddy energy confined more

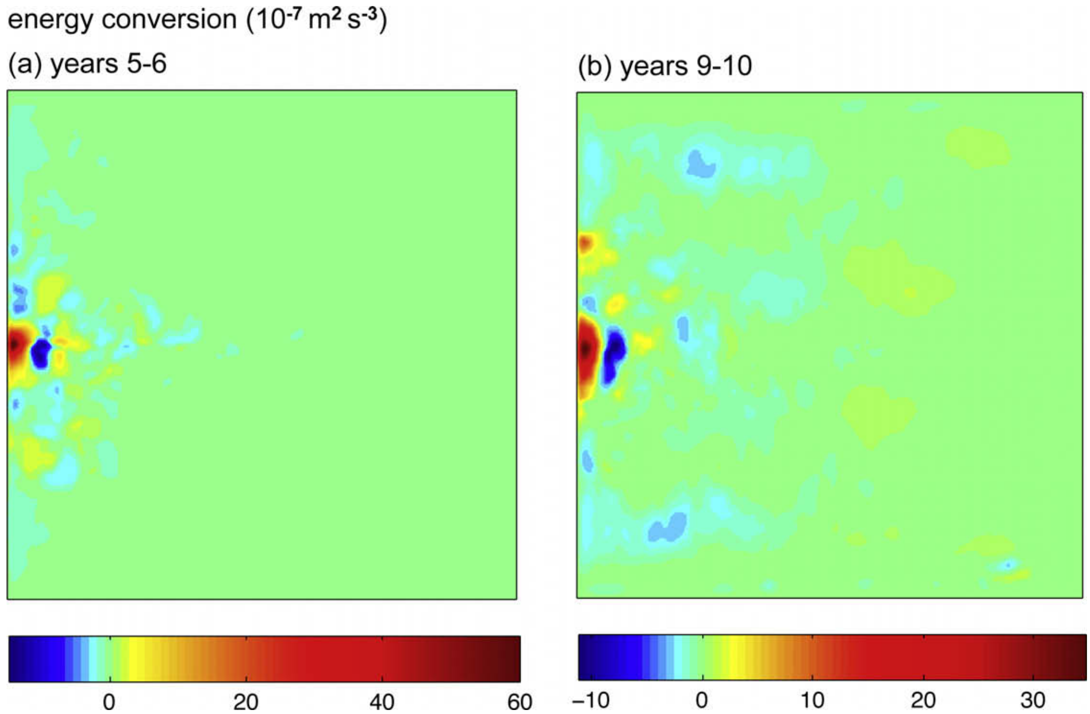

Fig. 4. The equivalent mean-to-eddy energy conversions terms as in (a) Fig. 2d and (b) Fig 3d, except calculated using the full eddy vorticity flux, i.e., $\overline{\mathbf{u}} \cdot \mathbf{k} \times \overline{q'\mathbf{u}'}$ (10^{-7} m^2 s^{-3}).

tightly to the western boundary. The main reason for these differences is the different location of the mean-to-eddy energy conversion in the no-slip solution (panel (d)). With no-slip boundary conditions, the region of largest negative $\partial q/\partial\psi_\perp$ is in the no-slip boundary layer, and hence this is where the greatest eddy energy growth is found. In contrast to the free-slip solution, there is relatively little back-scatter of eddy energy to the mean flow.

The mean fields are plotted in Fig. 6, averaged over years 9 and 10 of the equivalent eddy-resolving integration. The mean-to-eddy energy conversion is again defined using the divergent component of the eddy vorticity flux as in (19). There is a remarkably strong qualitative similarity between the energy conversion terms in the integrations with parameterized and explicit eddies, with the largest values being obtained in the no-slip boundaries layers, albeit with the magnitude of the energy conversion being roughly a factor of two larger in the case with explicit eddies. The eddy energy is also significantly enhanced adjacent to the western boundary both with parameterized and explicit eddies, consistent with the spatial patterns of mean-to-eddy energy conversion.

As in the free-slip eddy-resolving integration, there is some evidence of inertial Fofonoff gyres forming at the northern and southern limits of the domain, though these Fofonoff gyres are substantially weaker in the present case. Also curious is the emergence of a narrow strip of enhanced eddy energy adjacent to the northern and southern boundaries in the eddy-resolving integration. This initially forms near the western boundary, and extends increasingly eastward as the integration progresses through eddy energy dispersion. We have not been able to find similar behaviour in any integrations with parameterized eddy energy.

For both free-slip and no-slip boundary conditions, we have calculated solutions for a wide range of model parameters. The detailed patterns of the eddy energy change with the rates of eddy energy diffusion, dissipation, the choice of relation between the eddy energy and eddy diffusivity, including the proportionality constants, and with associated changes to the mean flow. However, the result that the mean-to-eddy energy conversion term is largest in relatively localized regions either at the inter-gyre boundary (for free-slip and some no-slip solutions) and adjacent to the western boundary (for no-slip and to a lesser extent free-slip solutions) appears to be robust across a wide range of parameters.

4.4. Freely-decaying turbulence

A particularly attractive property of the eddy parameterization considered in this paper is that it allows potential vorticity to be mixed without creating a spurious energy source. It is therefore one of the first eddy closures of which we are aware that is capable of parameterizing freely-decaying geostrophic turbulence. In this section, we present a solution to illustrate this concept, initialized with a uniform eddy kinetic energy of 0.1 m^2 s^{-2} that is subsequently allowed to "decay". Following Bretherton and Haidvogel (1976), Salmon et al. (1976), Cummins (1992) and Wang and Vallis (1994), we should expect mean flow to become established, consisting of two Fofonoff (1954) gyres, anticyclonic to the north and cyclonic to the south. This behaviour is associated with the direct cascade of enstrophy which is dissipated (equivalent to vorticity being mixed) and the inverse cascade of energy which is back-scattered to the mean flow.

The model parameters are identical to the wind-driven solutions, except that we exclude wind forcing and explicit dissipation of eddy energy (i.e., $r = 0$). We implement an alternative lateral boundary condition in which the net flux of vorticity through the boundary vanishes, somewhat analagous to the superslip and hyperslip boundary conditions included in some wind-driven gyre models (e.g., see Pedlosky, 1996). As found by Wang and Vallis (1994), the emergence of Fofonoff gyres is particularly sensitive to the nature of the lateral boundary condition, with no-slip conditions being most efficient at dissipating these boundary dominated flows. The emergence of substantial Fofonoff gyres in our parameterized model appears to rely on the implementation of slippery boundary conditions.

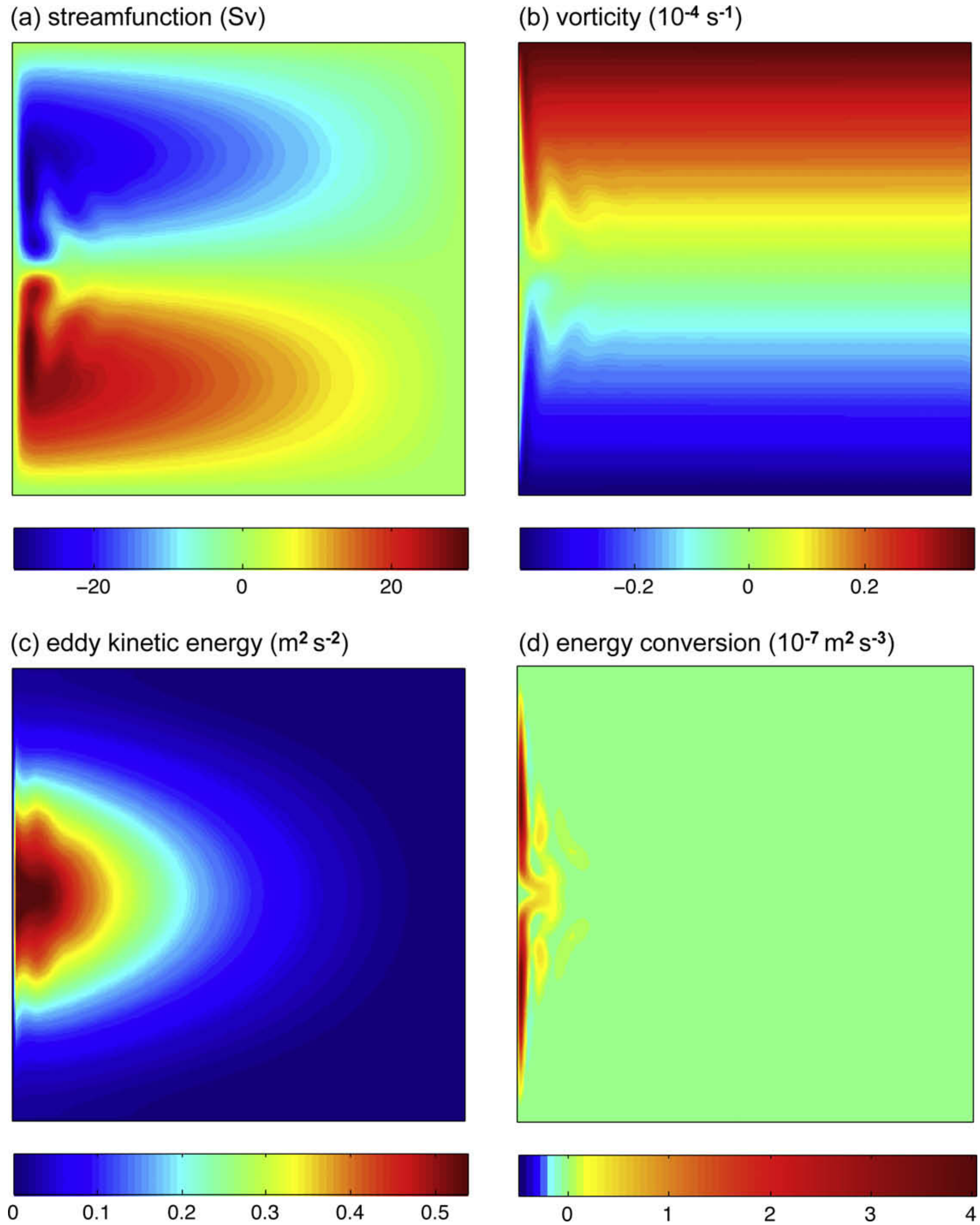

Fig. 5. Wind-driven gyres with no-slip boundary conditions and parameterized eddies. The panels show snapshots, after 10 years of integration from a rest state, of: (a) transport streamfunction, $H\psi$ (Sv); (b) absolute vorticity ($10^{-4}\ \mathrm{s}^{-1}$); (c) parameterized eddy kinetic energy ($\mathrm{m}^2\ \mathrm{s}^{-2}$); (d) mean-to-eddy energy conversion, $-\kappa\nabla\psi\cdot\nabla q$ ($10^{-7}\ \mathrm{m}^2\ \mathrm{s}^{-3}$).

In Figs. 7 and 8 we show the solutions after 5 and 10 years of model integration. After 5 years, intense recirculation gyres in excess of 65 Sv have formed at the northern and southern boundaries. These are associated with a reduction of the vorticity gradients in these regions – in fact $\partial q/\partial\psi_\perp$ becomes weakly positive. The eddy kinetic energy is greatly reduced over the region occupied by the gyres, to less than 40% of its initial value, compared with the central latitude where roughly 70% of the initial energy remains. While there are some regions of weak mean-to-eddy energy transfer, the dominant energy transfer is from the parameterized eddies to the mean flow, in a relatively wide band (compared with Figs. 1(d) and 5(d)), wrapping around the gyres (where the flow speed is large and $\partial q/\partial\psi_\perp > 0$). After 10 years, the gyres have strengthened to roughly 100 Sv and broadened to occupy a slightly wider latitude range. The eddy kinetic energy has reduced to around 25% of its initial value over the central latitude (being largest near the eastern boundary) and to less than 10% of its initial value within the Fofonoff gyres. The mean-to-eddy energy conversion is also reduced, concomitant with the reduction in eddy energy.

The character of the solution shown in Figs. 7 and 8 is broadly consistent with the eddy-resolving calculations reported in Wang and Vallis (1994). One such eddy-resolving calculation is presented here, again with $r = 0$ consistent with the absence of eddy energy

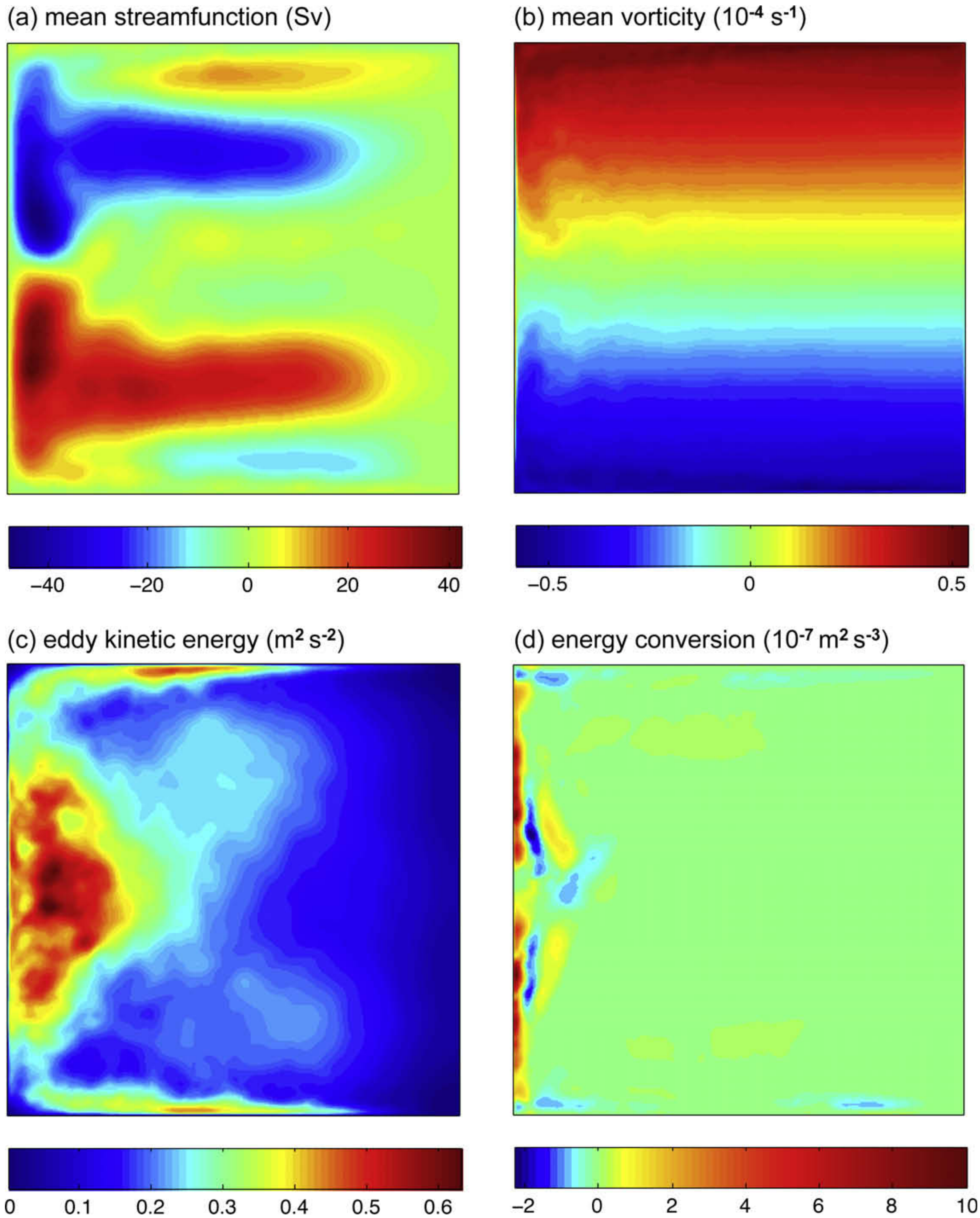

Fig. 6. Wind-driven gyres with no-slip boundary conditions and explicit eddies. The panels show a 2 year average over years 9–10 of integration from a rest state, of: (a) transport streamfunction, $H\overline{\psi}$ (Sv); (b) absolute vorticity (10^{-4} s^{-1}); (c) eddy kinetic energy (m^2 s^{-2}); (d) mean-to-eddy energy conversion, $\overline{\mathbf{u}}\cdot\mathbf{k}\times\overline{q'\mathbf{u}'}_{\rm div}$ (10^{-7} m^2 s^{-3}).

dissipation in the integration with parameterized eddies. The model is initialized with a random eddy field with a basin-averaged eddy kinetic energy equal to 0.1 $m^2\,s^{-2}$ (consistent with the preceding integration with parameterized eddy energy). The Fofonoff gyres emerge somewhat more rapidly in the eddy-resolving solution; accordingly, in Figs. 9 and 10 we show the equivalent fields averaged over years 1–2 and years 5–6.

Over the initial time-interval, years 1–2 (Fig. 9), the mean streamfunction already reveals gyres of strength 40–50 Sv. In contrast to the parameterized case, the eddy energy is enhanced on the western side of the basin at middle latitudes and depleted at the east, due to westward propagation of eddy energy (e.g., Chelton et al., 2007) which is not included in the parameterized model. However, over the regions occupied by the gyres, the eddy energy is greatly reduced, consistent with the parameterized model; the only exception is a narrow strip of eddy energy in the eddy-resolving case, immediately adjacent to the northern and southern boundaries. The mean-to-eddy energy conversion exhibits a complex spatial structure, but is negative on average, with largest negative values being found over the regions occupied by the Fofonoff gyres, as in the parameterized case. The net eddy-to-mean energy conversion is somewhat larger than in the parameterized case, consistent with faster growth of the Fofonoff gyres.

Over the latter time interval, years 5–6 (Fig. 10), the Fofonoff gyres have strengthened to roughly 65 Sv and the eddy energy has decayed to less than 10% of its initial value over these regions

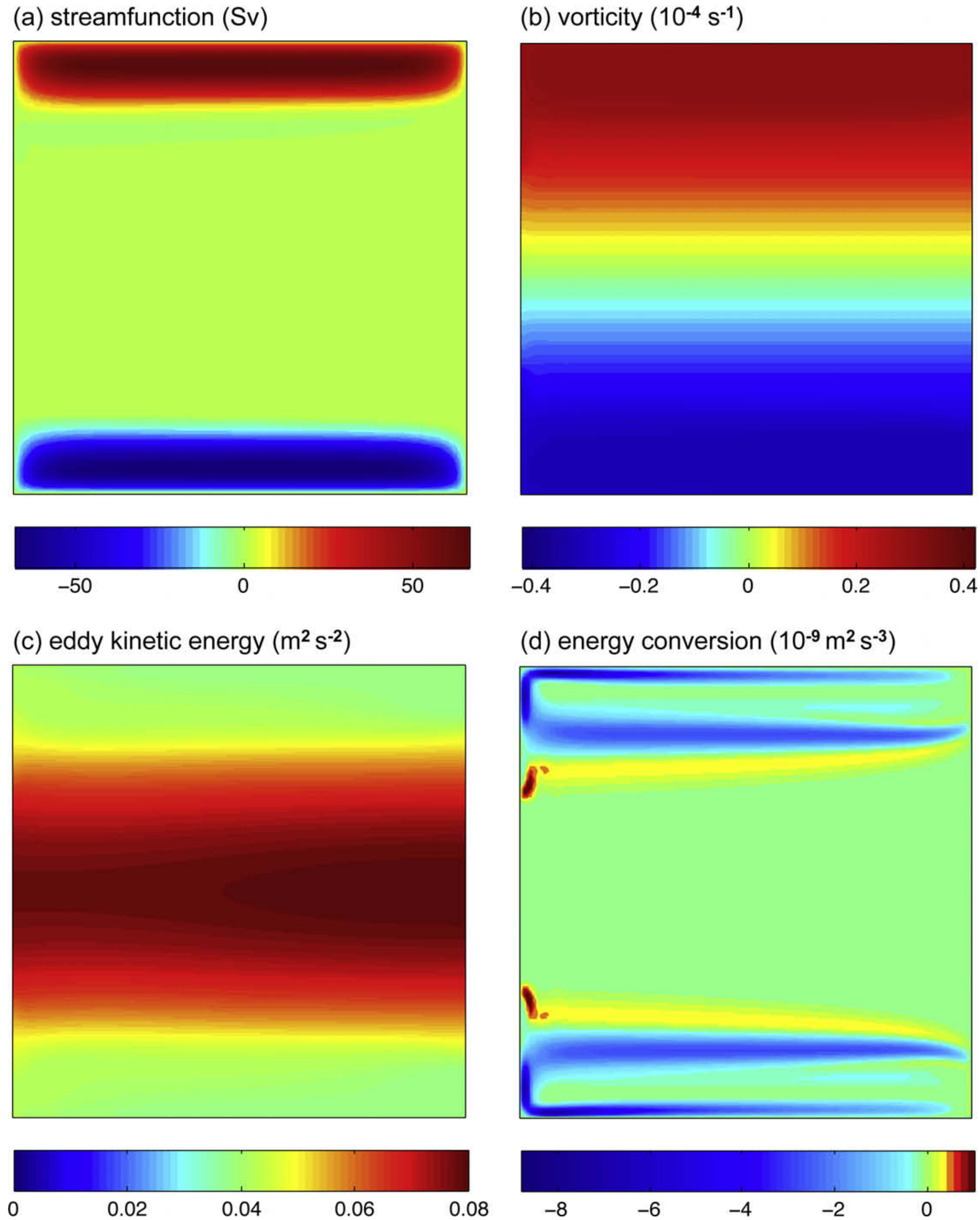

Fig. 7. Freely-decaying turbulence with parameterized eddies, after 5 years of integration from an initially uniform parameterized eddy kinetic energy. The panels show snapshots of: (a) transport streamfunction, $H\psi$ (Sv); (b) absolute vorticity (10^{-4} s^{-1}); (c) parameterized eddy kinetic energy (10^{-2} m^2 s^{-2}); (d) mean-to-eddy energy conversion, $-\kappa\nabla\psi\cdot\nabla q$ (10^{-9} m^2 s^{-3}).

(including on the northern and southern boundaries). The main difference with the parameterized case is a narrow strip of enhanced eddy energy, immediately flanking the inertial Fofonoff gyres; these strips of enhanced eddy energy appear to be associated with a localized region of mean-to-eddy energy conversion at the eastern margin of the Fofonoff gyres, indeed westward propagating eddies can be observed radiating from these regions in the transient solution (not shown).

Finally, in Fig. 11 we show the domain-averaged energy budget for the freely-decaying turbulence integrations with both parameterized and explicit eddies. Additionally plotted is the energy budget for an integration with parameterized eddies in which the eddy diffusivity for vorticity is maintained at a uniform, constant value, equal to the initial value in the standard case with parameterized eddy energy. With both parameterized and explicit eddies, the eddy energy initially grows at the expense of the eddy energy while the total energy decays slightly due to friction (somewhat more in the case with explicit eddies). The growth of the mean energy tapers off after about 10 years in the parameterized case, and after about 5 years in the eddy-resolving case; a notable difference is that significant eddy energy remains in the eddy-resolving calculation even after the Fofonoff gyres have achieved their maximum strength, mostly associated with the band of eddies flanking the Fofonoff gyres in the eddy-resolving calculation as discussed

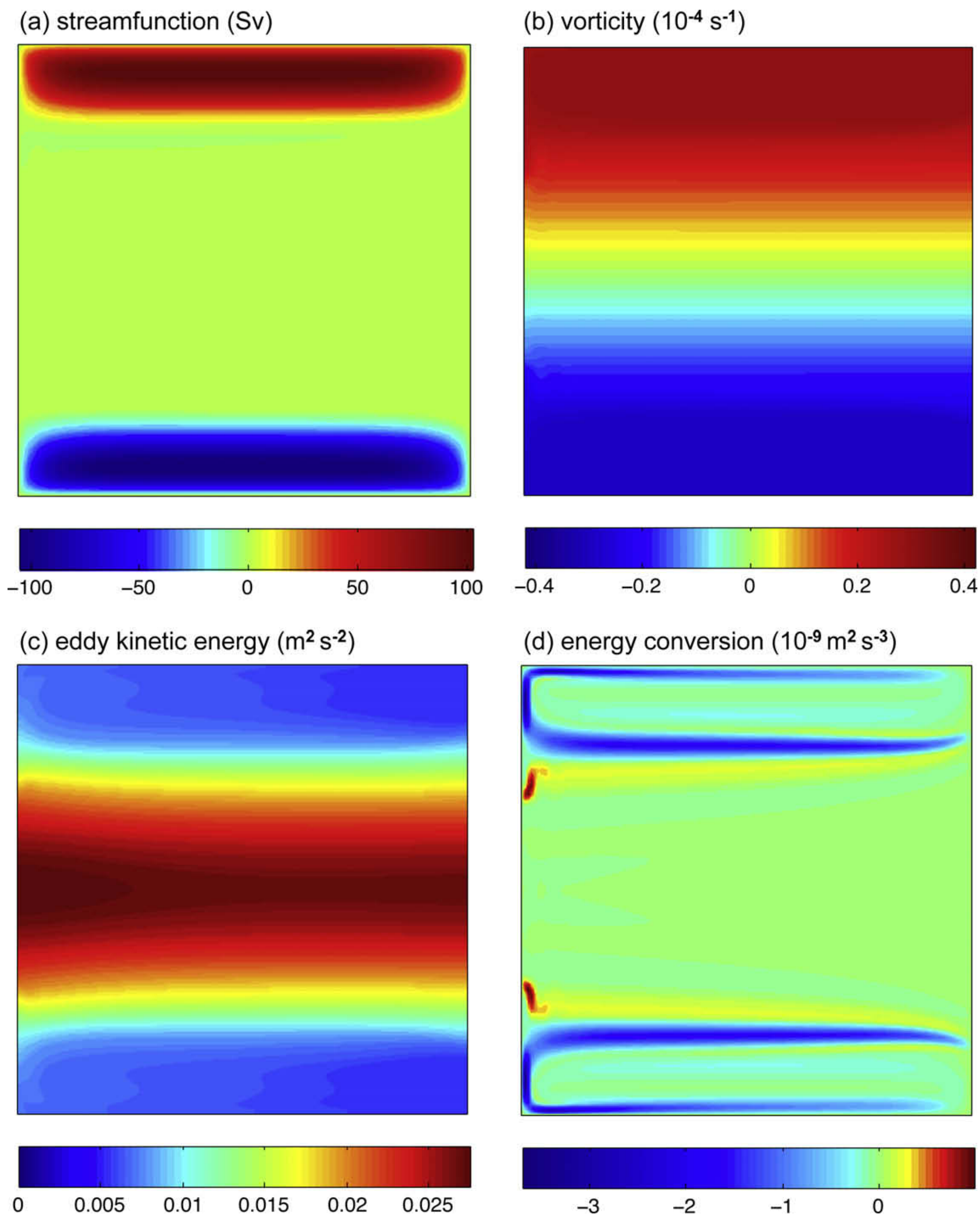

Fig. 8. As in Fig. 7 but after 10 years of integration.

above. In contrast, in the scenario in which the parameterized eddy diffusivity for vorticity is maintained at its initial value, the mean energy grows to a value far exceeding the energy available in the initial eddy field. Energy conservation thus places an unambiguous upper bound in these integrations of the amount of vorticity mixing that is permissible, set by the magnitude of the initial (parameterized or explicit) eddy energy.

5. Parameterized analogue of Arnold's first stability condition for a stratified, quasigeostrophic ocean

Finally we show that the parameterized analogue of Arnold's stability condition for the growth or decay of the parameterized eddy energy generalizes in a straightforward manner to a downgradient potential vorticity closure in a stratified, quasigeostrophic ocean.

5.1. Equations of motion and eddy fluxes

The time-filtered momentum and buoyancy equations for a stratified, quasigeostrophic ocean can be written:

$$\frac{\partial \mathbf{u}_g}{\partial t} + \mathbf{k} \times (f + \zeta)\mathbf{u}_g + \nabla B + f_0 \mathbf{k} \times \mathbf{u}_{ag} = -\mathbf{k} \times \overline{\zeta' \mathbf{u}'} - \nabla \frac{\overline{\mathbf{u}' \cdot \mathbf{u}'}}{2}, \quad (20)$$

$$\frac{\partial b}{\partial t} + \mathbf{u}_g \cdot \nabla b + wN^2 = -\nabla \cdot \overline{b' \mathbf{u}'}, \quad (21)$$

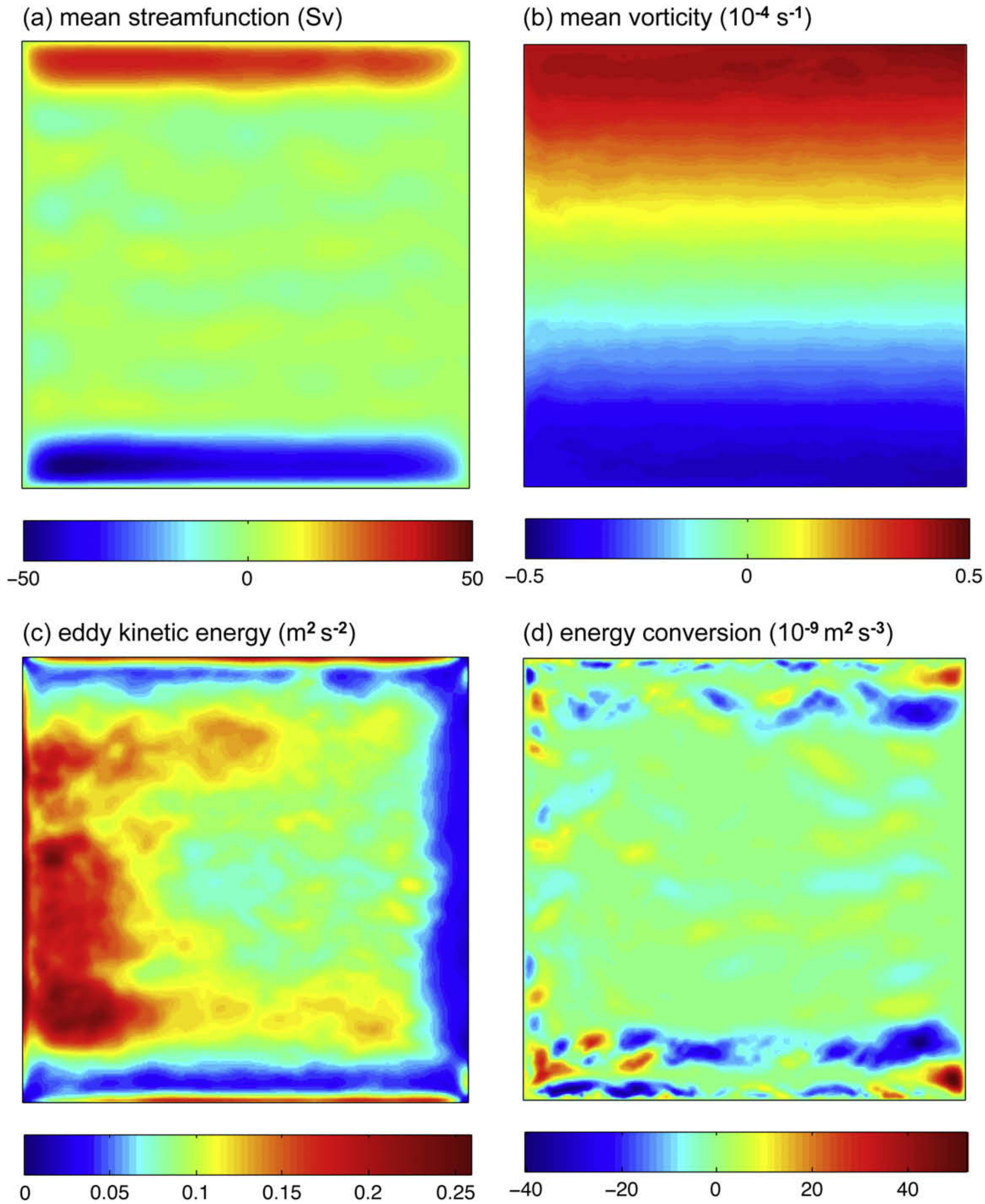

Fig. 9. Freely-decaying turbulence with explicit eddies. The panels show a 2 year average over years 1–2 of integration of: (a) transport streamfunction, $H\overline{\psi}$ (Sv); (b) absolute vorticity (10^{-4} s^{-1}); (c) eddy kinetic energy (10^{-2} m^2 s^{-2}); (d) mean-to-eddy energy conversion, $\overline{\mathbf{u}} \cdot \mathbf{k} \times \overline{q'\mathbf{u}'}_{\mathrm{div}}$ (10^{-9} m^2 s^{-3}).

here:

$$\mathbf{u}_g = \mathbf{k} \times \nabla\psi, \quad b = f_0 \frac{\partial \psi}{\partial z},$$

are the geostrophic velocity and buoyancy, where ψ is the streamfunction;

$$B = \frac{\mathbf{u}_g \cdot \mathbf{u}_g}{2} + \frac{p}{\rho_0}, \quad \zeta = \mathbf{k} \cdot \nabla \times \mathbf{u}_g, \quad f = f_0 + \beta y,$$

are the Bernoulli potential, relative vorticity and Coriolis parameter, where p is pressure, ρ_0 is the reference density, and f_0 and β are constants; and the ageostrophic velocity satisfies the continuity equation,

$$\nabla \cdot \mathbf{u}_{ag} + \frac{\partial w}{\partial z} = 0.$$

A formal derivation of the quasigeostrophic equations can be found in standard texts such as Pedlosky (1987) or Vallis (2006).

It follows that the evolution of the fluid motion is completely determined by the potential vorticity equation:

$$\left(\frac{\partial}{\partial t} + \mathbf{u}_g \cdot \nabla\right) Q = -\nabla \cdot \overline{Q'\mathbf{u}'}, \tag{22}$$

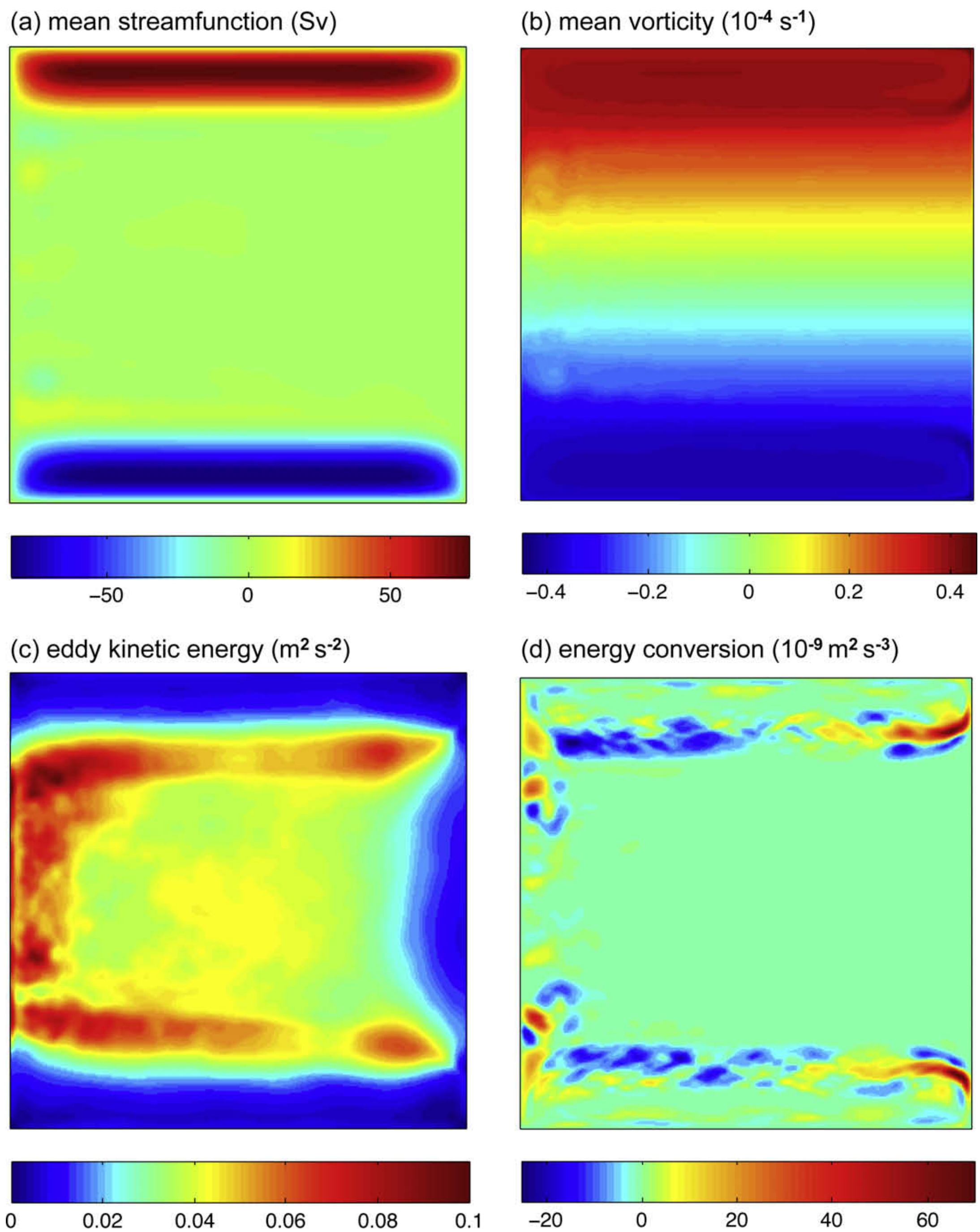

Fig. 10. As in Fig. 9 but averaged over years 5–6 of the integration.

where the quasigeostrophic potential vorticity is defined:

$$Q = \beta y + \zeta + \frac{\partial}{\partial z}\left(\frac{f_0}{N^2} b\right).$$

Surface and bottom boundaries are most conveniently considered as constant buoyancy, with actual boundary buoyancy variations instead being represented as delta-sheets of potential vorticity, following the procedure described by Bretherton (1966).

By analogy with the barotropic case, we assume a down-gradient closure for the eddy flux of potential vorticity, to within an arbitrary rotational gauge:

$$\overline{Q'\mathbf{u}'} = -\kappa \nabla Q + \mathbf{k} \times \nabla \lambda. \tag{23}$$

5.2. Energetics and Arnold's first stability condition

The quasigesotrophic energy equation can be written:

$$\frac{\partial}{\partial t}\left(\frac{\overline{\mathbf{u}' \cdot \mathbf{u}'}}{2} + \frac{\overline{b'^2}}{2N^2}\right) = \mathbf{k} \times \overline{\mathbf{Q}'\mathbf{u}'} \cdot \mathbf{u} + \nabla \cdot (\ldots)$$

$$= -\kappa \nabla Q \cdot \nabla \psi + \nabla \cdot (\ldots) \tag{24}$$

$$= -\kappa \frac{\partial Q}{\partial \psi_\perp} \mathbf{u} \cdot \mathbf{u} + \nabla \cdot (\ldots) \tag{25}$$

where

$$\frac{\partial Q}{\partial \psi_\perp} = \frac{\nabla Q \cdot \nabla \psi}{\nabla \psi \cdot \nabla \psi}.$$

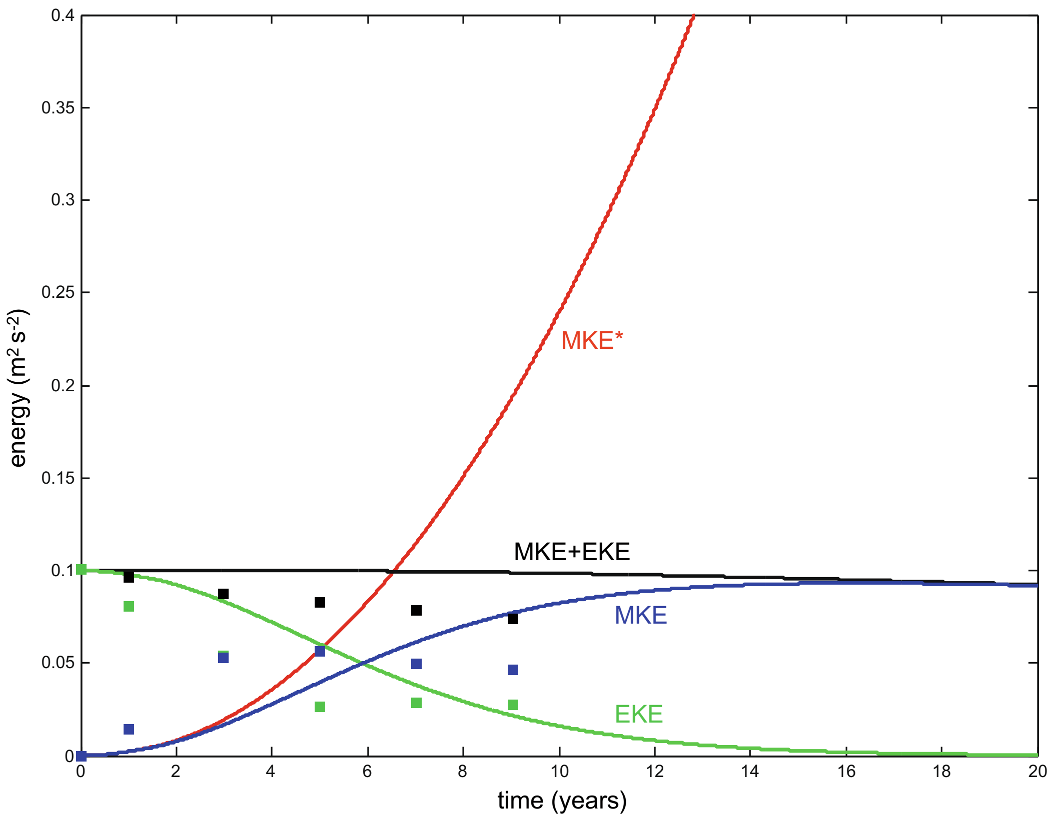

Fig. 11. Time series of the basin-averaged mean (MKE, blue), eddy (EKE, green) and total kinetic energy (MKE + EKE, black) from the freely-decaying turbulence integrations shown in Figs. 7–10. The solid lines show the energy budget for the integration with parameterized eddies (Figs. 7 and 8) and the solid squares the two year averages from the eddy-resolving integration (Figs. 9 and 10). The latter also includes a point at time 0 where it is assumed that all of the energy is in eddy form. Also shown is the mean kinetic energy (MKE*, red) from an integration in which the eddy diffusivity for vorticity is maintained at its initial value and no consistent eddy energy budget is solved. (For interpretation of the references to color in this figure legend, the reader is referred to the web version of this article.)

Thus, as in the barotropic limit, there is a precise connection between the net decay or growth of the parameterized eddy energy and the stability or instability of the flow, analogous to Arnold's first stability theorem. Specifically, if $\partial Q/\partial \psi_\perp$ is everywhere positive, which is a sufficient condition for stability, then the parameterized eddy energy decays on average and is converted to mean energy; conversely, if $\partial Q/\partial \psi_\perp$ is somewhere negative, which is a necessary condition for instability, then the parameterized eddy energy might be able to grow on average at the expense of mean energy.

6. Discussion

Stability properties of fluid flows are often associated with conservation principles. In this manuscript, we have studied the stability properties of a class of eddy closures that (i) flux (potential) vorticity down-gradient, and (ii) solve an explicit conservation equation for the parameterized eddy energy, as proposed by Eden and Greatbatch (2008). We have shown that such closures preserve a parameterized analogue of Arnold's first stability theorem: the growth or decay of the eddy energy is related to the sign of $\partial Q/\partial \psi_\perp$ where Q is the potential vorticity, ψ is the streamfunction, and the derivative is evaluated perpendicular to the streamlines. Specifically $\partial Q/\partial \psi_\perp > 0$ everywhere is a sufficient condition for stability and for the parameterized eddy energy to decay on average; conversely $\partial Q/\partial \psi_\perp < 0$ somewhere is a necessary condition for instability and for the parameterized eddy energy to grow on average. These results have been derived for barotropic and quasigeostrophic stratified oceans, but we have no reason to assume they are specific to these settings.

A practical benefit of solving a prognostic eddy energy equation is that it allows potential vorticity to be fluxed down-gradient without generating spurious sources of energy. This has been a particularly problematic issue over variable bottom topography where complete potential vorticity homogenization (including the contribution from the bottom density variations) requires the isopycnals to rise completely over the topography. Attempts to flux potential vorticity down-gradient in such regions (e.g., Greatbatch and Li, 2000) can therefore result in unphysically large topographic recirculations and imply spurious energy sources. Adcock and Marshall (2000) proposed a potential vorticity closure which conserves the energy of the resolved flow in order to avoid these spurious energy sources. However, the present approach offers a more practical and physically consistent solution in which the eddy energy, and hence the potential vorticity fluxes, decay as energy is transferred from the eddies to the mean flow.

One issue that we have not addressed here, but is discussed briefly in Eden and Greatbatch (2008), is the role of angular momentum conservation in multiply-connected domains. Angular momentum conservation imposes additional constraints on the eddy fluxes of potential vorticity (e.g., Green, 1970; Marshall, 1981; Wood and McIntyre, in press), which are generally incompatible with fluxing potential vorticity down-gradient while relating the eddy transfer coefficient solely to the eddy energy. Eden and Greatbatch discuss the pragmatic solution of adding an additional term to the eddy potential vorticity flux to restore angular momentum conservation, but this approach destroys some of the relations we have derived here between the stability properties of the flow and the growth or decay of eddy energy. Instead, we suspect that it is necessary to parameterize the eddy potential vorticity flux in a manner that preserves the symmetry properties of the original equations leading to angular momentum conservation. Preliminary results suggest that the relation between Arnold's stability condition and the growth or decay of the parameterized eddy energy is preserved when angular momentum in conserved in this manner; these results will be reported in detail in a future manuscript.

Finally, we note that the detailed nature of the model solutions can be sensitive to parameterizations of the dispersion of eddy energy. In the present manuscript, the eddy energy has been simply diffused and advected by the mean flow, following Eden and Greatbatch (2008). However, it is clear from satellite observations that there is a westward propagation of eddy energy in the ocean, at roughly the long Rossby wave speed for the first baroclinic mode (Chelton et al., 2007). There is also the important issue of how energy is transferred in the vertical (for example, to the barotropic mode). Nevertheless, we should stress that the parameterized analogue of Arnold's first stability theorem applies only in an integral sense (as does the original form of Arnold's first stability theorem), and hence it is independent of how the eddy energy disperses.

Acknowledgments

We wish to thank Peter Killworth for his many creative and inspirational contributions to Physical Oceanography. In particular, we thank Peter for setting up this wonderful journal, the success of which testifies to Peter's vision, enthusiasm and hard work. DPM also wishes to thank Peter for the continuous support and encouragement he provided to a young researcher finding his way in UK Physical Oceanography. We are grateful to two anonymous reviewers whose detailed and insightful comments led to a greatly improved manuscript, and to Anand Gnanadesikan for a careful reading of the final manuscript. DPM acknowledges the financial support of the Natural Environment Research Council.

References

Adcock, S., Marshall, D.P., 2000. Interactions between geostrophic eddies and the mean circulation over large-scale bottom topography. J. Phys. Oceanogr. 30, 3232–3238.

Arbic, B.K., Scott, R.B., 2008. On quadratic bottom drag, geostrophic turbulence, and oceanic mesoscale eddies. J. Phys. Oceanogr. 38, 84–103.

Arnold, V.I., 1965. Conditions for nonlinear stability of stationary plane curvilinear flows of an ideal fluid. Dokl. Akad. Nauk. SSSR. 162, 975–978.

Berloff, P.S., McWilliams, J.C., 1999. Quasigeostrophic dynamics of the western boundary current. J. Phys. Oceanogr. 29, 2607–2634.

Bretherton, F.P., 1966. Critical layer instability in baroclinic flows. Q. J. Roy. Meteorol. Soc. 92, 325–334.

Bretherton, F.B., Haidvogel, D., 1976. Two-dimensional turbulence over topography. J. Fluid Mech. 78, 129–154.

Bryan, K., 1969. A numerical method for the study of the circulation of the world ocean. J. Comp. Phys. 4, 347–376.

Canuto, V.M., Dubovikov, M.S., 2005. Modeling mesoscale eddies. Ocean Modell. 8, 1–30.

Canuto, V.M., Dubovikov, M.S., 2006. Dynamical model of mesoscales in *z*-coordinates. Ocean Modell. 11, 123–166.

Capet, X., McWilliams, J.C., Molemaker, M.J., Shchepetkin, A.F., 2008. Mesoscale to submesoscale transition in the California current system. Part II: frontal processes. J. Phys. Oceanogr. 38, 44–64.

Cessi, P., 2008. An energy-constrained parametrization of eddy buoyancy flux. J. Phys. Oceanogr. 38, 1807–1819.

Chelton, D.B., Schlax, M.G., Samelson, R.M., de Szoeke, R.A., 2007. Global observations of large oceanic eddies. Geophys. Res. Lett. 34, L15606. doi:10.1029/2007GL030812.

Cummins, P.F., 1992. Inertial gyres in decaying and forced geostrophic turbulence. J. Mar. Res. 50, 545–566.

Danabasoglu, G., McWilliams, J.C., Gent, P.R., 1994. The role of mesoscale tracer transports in the global ocean circulation. Science 264, 1123–1126.

Duhant, T.H., Straub, D.N., 2006. Wind stress dependence on ocean surface velocity: implications for mechanical energy input to ocean circulation. J. Phys. Oceanogr. 36, 202–211.

Eden, C., Greatbatch, R.J., 2008. Towards a mesoscale eddy closure. Ocean Modell. 20, 223–239.

Fofonoff, N.P., 1954. Steady flow in a frictionless homogeneous ocean. J. Mar. Res. 13, 254–262.

Gent, P.R., McWilliams, J.C., 1990. Isopycnal mixing in ocean circulation models. J. Phys. Oceanogr. 20, 150–155.

Gent, P.R., Willebrand, J., McDougall, T.J., McWilliams, J.C., 1995. Parameterizing eddy-induced tracer transports in ocean circulation models. J. Phys. Oceanogr. 25, 463–474.

Greatbatch, R.J., Li, G., 2000. Alongslope mean flow and an associated upslope bolus flux of tracer in a parameterization of mesoscale turbulence. Deep Sea Res. Part I 47, 709–735.

Greatbatch, R.J., Nadiga, B.T., 2000. Four-gyre circulation in a barotropic model with double-gyre wind forcing. J. Phys. Oceanogr. 30, 1461–1471.

Green, J.S.A., 1970. Transfer properties of the large-scale eddies and the general circulation of the atmosphere. Q. J. Roy. Meteorol. Soc. 96, 157–185.

Holland, W.R., Rhines, P.B., 1980. An example of eddy-induced circulation. J. Phys. Oceanogr. 10, 1010–1031.

Holloway, G., 1987. Systematic forcing of large-scale geophysical flows by eddy-topography interaction. J. Fluid Mech. 184, 463–476.

Holm, D.D., Wingate, B.A., 2005. Baroclinic instabilities of the two-layer quasigeostrophic alpha model. J. Phys. Oceanogr. 35, 1287–1296.

Hughes, C.W., Ash, E., 2001. Eddy forcing of the mean flow in the Southern Ocean. J. Geophys. Res. 106, 2713–2722.

Killworth, P.D., 1997. On the parameterization of eddy transfer. Part I. Theory. J. Mar. Res. 55, 1171–1197.

Killworth, P.D., 1998. On the parameterization of eddy transfer, Part II: tests with a channel model. J. Mar. Res. 56, 349374.

Killworth, P.D., 2001. Boundary conditions on quasi-Stokes velocities in parameterizations. J. Phys. Oceanogr. 31, 1132–1155.

Killworth, P.D., 2005. Parameterization of eddy effects on mixed layers and tracer transport: a linearized eddy perspective. J. Phys. Oceanogr. 35, 1711–1725.

Marshall, J.C., 1981. On the parameterization of geostrophic eddies in the ocean. J. Phys. Oceanog. 11, 1257–1271.

Marshall, D., Marshall, J., 1992. Zonal penetration scale of midlatitude oceanic jets. J. Phys. Oceanogr. 22, 1018–1032.

Marshall, D.P., Naveira Garabato, A.C., 2008. A conjecture on the role of bottom-enhanced diapycnal mixing in the parameterization of geostrophic eddies. J. Phys. Oceanogr. 38, 1607–1613.

Marshall, J.C., Shutts, G.J., 1981. A note on rotational and divergent eddy fluxes. J. Phys. Oceanogr. 11, 1677–1680.

Pedlosky, J., 1987. Geophysical Fluid Dynamics. Springer-Verlag. 710 pp.

Pedlosky, J., 1996. Ocean Circulation Theory. Springer-Verlag. 453pp.

Polzin, K.L., 2008. Mesoscale eddyinternal wave coupling. Part I: symmetry, wave capture, and results from the mid-ocean dynamics experiment. J. Phys. Oceanogr. 38, 2556–2574.

Rhines, P., 1975. Waves and turbulence on a beta-plane. J. Fluid Mech. 69, 417–443.

Rhines, P.B., Young, W.R., 1982. Homogenization of potential vorticity in planetary gyres. J. Fluid Mech. 122, 347–367.

Roberts, M.J., Marshall, D.P., 2000. On the validity of down-gradient eddy closures in ocean models. J. Geophys. Res. 105, 28613–28628.

Sadorny, R., Basdevant, C., 1985. Parameterization of subgrid scale barotropic and baroclinic eddies in quasi-geostrophic models: anticipated potential vorticity method. J. Atmos. Sci. 42, 1353–1363.

Salmon, R., 1998. Lectures on Geophysical Fluid Dynamics. Oxford University Press. 400 pp.

Salmon, R., Holloway, G., Hendershott, M., 1976. The equilibrium statistical mechanics of simple quasigeostrophic models. J. Fluid Mech. 75, 691–703.

Stone, P., 1972. A simplified radiative-dynamical model for the static stability of the rotating atmosphere. J. Atmos. Sci. 29, 405–418.

Tandon, A., Garrett, T., 1996. On a recent parameterization of mesoscale eddies. J. Phys. Oceanogr. 26, 406–411.

Tansley, C.E., Marshall, D.P., 2001. Flow past a cylinder on a β plane, with application to Gulf Stream separation and the Antarctic Circumpolar Current. J. Phys. Oceanogr. 31, 3274–3283.

Vallis, G.K., 2006. Atmospheric and Oceanic Fluid Dynamics. Cambridge University Press. 745 pp.

Vallis, G.K., Hua, B.L., 1988. Eddy viscosity of the anticipated potential vorticity method. J. Atmos. Sci. 45, 617–627.

Visbeck, M., Marshall, J., Haine, T., Spall, M., 1997. On the specification of eddy transfer coefficients in coarse resolution ocean circulation models. J. Phys. Oceanogr. 27, 381–402.

Wang, J., Vallis, G.K., 1994. Emergence of Fofonoff states in inviscid and viscous ocean circulation models. J. Mar. Res. 52, 83–127.

Williams, G.P., 1978. Planetary circulations: I. Barotropic representation of Jovian and terrestrial turbulence. J. Atmos. Sci. 35, 1399–1426.

Wood, R.B., McIntyre, M.E., in press. A general theorem on angular-momentum changes due to potential vorticity mixing and on potential-energy changes due to buoyancy mixing. J. Atmos. Sci.

Zhai, X., Greatbatch, R.J., 2007. Wind work in a model of the Atlantic Ocean. Geophys. Res. Lett. 34, L04606. doi:10.1029/2006GL028907.